Journal of Engineering and Technology Research Vol.1 (8), pp. 152-170, November, 2009
Available online at http://www.academicjournals.org/jetr
ISSN 2006-9790© 2009 Academic Journals

Full Length Research Paper

Thermal stresses in a plate with hyperelliptical hole

S. K. Bhullar* and J. L. Wegner

Department of Mechanical Engineering, University of Victoria, PO Box 3055, Victoria, B.C. Canada V8W 3P6.

Accepted 4 September, 2009

The aim of this paper is to study the thermal stress analysis in a plate with a hole in a hyperelliptical shape assuming the state of plane stress. The system of stress is analyzed using complex variable method under isothermal conditions. The high stress concentration found at the edge of a hole is of great importance, therefore stress system at the tip and in the neighborhood of the tip of the hole are also studied. Numerical calculations are computed for material steel and contour graphs are depicted to show the obtained results.

Key words: Azimuthal stresses, complex variable method, thermal stresses, plane stress.

INTRODUCTION

Thermal stresses play an important role in the design of high speed flight vehicles, machine structures and also in the fields of nuclear and chemical engineering. It is essential to determine the magnitude and influence of these stresses to make a realistic design of such components. It is well known that in an infinite plate a steady heat flow with a constant temperature gradient (uniform heat flow) does not induce thermal stresses provided there is no hole in the plate and no mechanical constraints are present at the outer edges. Thermal stresses are induced, however, if the uniform heat flow is disturbed by the presence of an insulated hole or by the inclusion of another material.

Specifically one may encounter single or multiple holes of simple or arbitrary geometries in the plate. The objective of this research is to study the state of stress around a more general shape hole. For this purpose we are investigating hole of hyperelliptical geometry, in a plate, as it enables us to study a variety of shapes (Figure 1).

LITERATURE REVIEW

The investigation of stress concentration around holes and notches of arbitrary shape in a given elastic medium is very important for modern engineering. During the past few decades, widespread attention has been given to the thermal stress problems in an elastic medium with inclusion, holes or cracks. The heat generating cylinder with a hole is used in the construction of the reactor. The circular cylinder with a square hole is an applicable problem in the construction of support of the bridge. Polygon region with an elliptic hole have been used in nuclear reactor. The early work was started by Goodier and Florence (Goodier and Florence, 1959; Florence and Goodier, 1959; Florence and Goodier, 1960; Goodier and Florence, 1963; Florence and Goodier, 1962; Florence and Goodier, 1964) on localized thermal stress at holes, cavities and inclusions due to the disturbance of a uniform heat flow. The thermal stresses in thin elastic finite plates with insulated circular, elliptic and rectangular holes, the problem of thermal stress with internal heat generation in the square region with an elliptical hole at the centre are described in (Hoffman and Ariman, 1970; Rao et al., 1971; Matsumoto and Sekiya, 1982). Transient thermal stresses in an infinite plate with a circular hole due to a moving heat source, an analytical solution of elliptical cylindrical cavities and a general solution for two dimensional stress distributions around triangle holes in isotropic plate are studied in (Matsumoto and Sekiya, 1982; Goshima and Miyao, 1990; Hong and Kim, 1995; Ukadgaonker and Rao, 1999). A two-dimensional mixed boundary value problems for an anisotropic thermoelastic body containing an elliptic hole boundary and thermoelastic stress analysis used to obtain the stress concentration factors (SCFs) from a variety of circular holes in cylinders are presented in (Chao and Gao, 2001; Quinn and Dulieu-Barton, 2002). Temperature and thermal stresses in hexagon regions with a elliptic hole using

*Corresponding author. E-mail: sbhullar@uvic.ca.

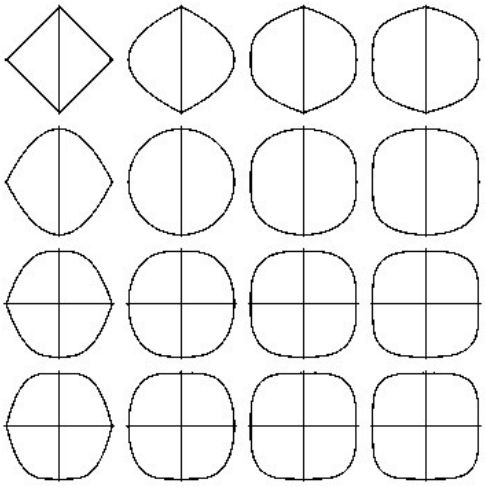

Figure 1. A variety of shapes of hyperelliptical hole.

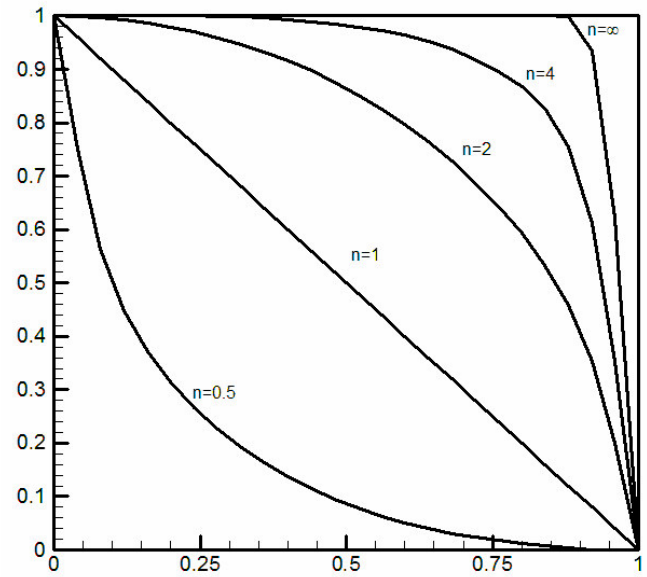

Figure 2. The effect of the geometric parameter *n* upon the shape of the hole in first quadrant.

elliptic co-ordinates, the distribution of stresses due to step input of temperature on the boundaries of a homogeneous transversely isotropic circular disc in the context of generalized theories of thermo-elasticity, a thermo-elastic solution to a coated elliptic hole embedded in an infinite plate subjected to a remote uniform heat flow, a general solution to a reinforced elliptic hole embedded in an infinite matrix subjected to a remote uniform load is provided in plane elasticity problems of an infinite plate weakened by a hole having arbitrary shape and a problem of thermoelastic interactions in an isotropic unbounded medium with cylindrical cavity due to the presence of moving heat sources in the context of the linear theory of generalized thermoelasticity with one relaxation time has been studied in (Bhullar, 2006; Kara and Kanoria, 2007; Chen and Chao, 2008; Abdou and Aseeri, 2009; Youssef, 2009). In the present paper state of stresses around hole of hyperelliptical geometry is studied.

FORMULATION OF PROBLEM

We have assumed an infinite plate in which a stationary stream of heat flows in the direction of y-*axis*. The origin *O*, of the coordinates *x, y* lies within the hole. The temperature of the plate at infinity is $\theta_\infty = qy$ with uniform heat flux q. The flow is disturbed by a hyperelliptical hole, bounded by a smooth thermally insulated contour, is described by the following equation:

$$\left(\frac{x}{a}\right)^n + \left(\frac{y}{b}\right)^n = 1,\ 0 \le n \le \infty \qquad (1)$$

Where;, *a* and *b* are the characteristic dimensions along the *x* and *y* axes respectively. The shape of plate depends on geometric parameter *n*, for *n* = 2, the shape of hole is elliptical if *a* > *b* or circular if *a* = *b*; for *n* = 1, the hole is diamond shape if *a* > *b* or square if *a* = *b*; for *n* > *2*, the shape is rectangle if *a* > *b* or a square if *a* = *b* with rounded corners (Figure 1). The effect of geometric parameter n upon the shape of the hole in first quadrant is shown in Figure 2.

METHOD OF SOLUTION

To study thermal stresses in the state of plane stress the generalized Kolosov equations which are the fundamental equations of the method of complex variables, are as following:

$$\tau_{xx} + \tau_{yy} = 2\left[\psi_1'(z) + \psi_2'(z)\right] - E\alpha\theta \qquad (2a)$$

$$\tau_{yy} - \tau_{xx} + 2\imath\tau xy = 2\left[z\psi_1''(z) + \chi''(z)\right] - E\alpha\int\frac{\partial\theta(z,\bar{z})}{\partial z}dz \qquad (2b)$$

where, *E* is young's modulus, α is linear thermal expansion, *ψ(z)* and *χ(z)* are thermoelastic potentials of complex variable *z = x + ıy* and *ψ(z)* and *χ(z)* the conjugates of *ψ(z)* and *χ(z)*. Boundary conditions are:

$$\psi_1(z) + z\psi_1'(z) - \chi'(\bar{z}) = F(x,y) = \frac{E\alpha}{2}\int\theta d\theta + C_1 \qquad (3)$$

Where; *F(x, y)* denotes the function of position. Also, for infinite plate $\psi_1(z)$ and *χ'(z)* can be represented by the relation

$$\psi_1(z) = -P + (B + \imath C) + \phi_0(z) \quad (4)$$

$$\chi'(z) = P + (B' + \imath C') + \chi_0(z) \quad (5)$$

$$P = \sum_{k=1}^{\infty} \frac{P_x + \imath P_y}{2\pi(1+k^*)} In\, z \quad (6)$$

Where; P_x , P_y , $k^* = \frac{3-\nu}{1+\nu}$ are the components of the resultant of the forces acting on the contour. *B, C, B'* and C′ are constants, $\phi_0(z)$, $\chi_0(z)$ are in form of :

$$\sum_{k=0}^{\infty} \frac{a_k}{z_k} \quad (7)$$

And a_k are in general complex. Under conformal mapping transformations first and second derivative of function *ψ(z)* are as follows:

$$\psi'(z) = d\psi[\omega(w)]\frac{dw}{dz} \quad (8)$$

$$= \psi'(w)\frac{1}{\omega'(w)} \quad (9)$$

$$\psi''(z) = \frac{d}{dw}\left[\frac{\psi'(w)}{\omega'(w)}\right]\frac{dw}{dz} \quad (10)$$

$$= \frac{\psi''(z)\omega'(w) - \psi(z)\omega''(w)}{[\omega'(w)]^3} \quad (11)$$

To map the complex plane with a hole of arbitrary shape onto the exterior of the unit circle, we have the mapping in the following form:

$$z = \omega(w) = R\left(w + \sum_{k=0}^{\infty} a_k w^{-k}\right), \ |w \geq 1| \quad (12)$$

Where; R is a constant. Substituting (12) in (4) and (5) and we get

$$\psi_1(w) = -P + (B + \imath C)w + \phi^*(w) \quad (13)$$

$$\chi'(w) = -k^* P + R(B' + \imath C')w + \phi^*(w) \quad (14)$$

$$P = \sum_{k=1}^{n} \frac{P_x + \imath P_y}{2\pi(1+k^*)} In\, w \quad (15)$$

$$\phi^*(w) = \sum_{k=0}^{\infty} a_k w^{-k} \quad (16)$$

$$\psi^*(w) = \sum_{k=0}^{\infty} b_k w^{-k} \quad (17)$$

Where; $|w| > 0$, $\phi^*(w)$ and $\psi^*(w)$ are two analytic functions. Upon making use of transformation of Cartesian co-ordinates *(x, y)* into curvilinear coordinates *(ρ, β),* we have modified equation (2a) - (2b) and we arrive at the following expressions:

$$\tau_{\rho\rho} + \tau_{\beta\beta} = 2\left[F_1(w) + \overline{F}_1(w)\right] - E\alpha\theta(w, \overline{w}) \quad (18a)$$

$$\tau_{\rho\rho} - \tau_{\beta\beta} + 2\imath\tau_{\rho\beta} = \frac{2w^2}{\rho^2\overline{\omega}'(w)}\left[\overline{\omega}(w)F_1'(w) + \omega'(w)F_2(w)\right] - \frac{E\alpha}{2}\int \overline{\omega}'(w)\frac{\partial\theta}{\partial w}d\overline{w} \quad 18b)$$

Since we are using method of complex variables and conformal mapping, it is imagined that the exterior of the hole is mapped conformally onto the exterior of the unit circle in the w-plane by means of the function $z = \omega(w)$. As a conformal mapping leaves a harmonic function harmonic, the temperature $\theta(\rho, \beta)$ in the *w-plane*, where $w = \rho e^{\imath\beta}$ satisfy the equation;

$$\frac{\partial^2\theta}{\partial\rho^2} + \frac{1}{\rho}\frac{\partial\theta}{\partial\rho} + \frac{1}{\rho^2}\frac{\partial^2\theta}{\partial\beta^2} = 0 \quad (19)$$

The temperature boundary conditions are;

$$\frac{\partial\theta}{\partial\rho} = 0, \ for \ \ \rho = 1, \quad (20a)$$

$$\theta = Rq\rho Sin\beta, \ for \ \rho = \infty \quad (20b)$$

Where; *R is* real parameter depending on form and dimensions of the hole in the z-plane. Upon assuming the separation of variables

$$\theta(\rho, \beta) = R^*(\rho)B(\beta) \quad (21)$$

We reduce the problem to solution of two ordinary differential equations

$$\rho^2 R^{*''} + \rho R^* - \lambda^2 = 0 \quad (22a)$$

$$B'' + \lambda^2 B = 0 \quad (22b)$$

Where; λ is a parameter to be determined from the boundary conditions. The solution of equation (22a)-(22b) is;

$$R^* = C_1\rho^{\lambda} + C_2\rho^{-\lambda} \quad (23a)$$

$$B = a\cos\lambda\beta + b\sin\lambda\beta \quad (23b)$$

Boundary condition equation 20(a) shows that $C_1 = C_2$, and in order for the remaining conditions to be satisfied identically, one must put λ = 1, a = 0, b = 1 and $C_1 = qR$. Hence,

$$\theta(\rho,\beta) = qR\left(\rho + \frac{1}{\rho}\right)\sin\beta \quad (24)$$

As $w = \rho e^{\iota\beta}$ and $e^{\pm\iota\frac{\pi}{2}} = \pm\iota$ and we can write equation (24) into the form

$$\theta(w,\overline{w}) = qR\iota\left[(\overline{w} - w) + \left(\frac{1}{w} - \frac{1}{\overline{w}}\right)\right] \quad (25)$$

APPLICATION

Although circular holes are widely used on account of their simple geometry, an elliptic hole is important because it may reduce the stress concentration and therefore prove advantageous. Therefore, first the problem of an infinite plate with an elliptic hole is studied. Further, most of the work exist in literature is on thermal stresses in a plate with square holes, second, the results for an unbounded plate with a square hole with smoothly rounded corners are obtained For this purpose we have investigated two different cases:

$n. > 2 \ \ and \ \ a = b$, $n. = 2 \ \ and \ \ a \neq b$

The equation for $n. > 2 \ \ and \ \ a = b$ represents a square hole with rounded corners. To study this case we consider an unbounded plate with a "square" hole centered at $z = 0$ with smoothly rounded corners and having axes of symmetry parallel to the co-ordinate axes. We are mapping exterior of square with rounded corners onto the interior of the unit circle $\sigma = e^{\iota\beta}$. The appropriate mapping function in this case is given by;

$$z = R\left(w - \frac{1}{6w^3}\right) \quad (26)$$

It is assumed the plate is free from external load. Upon substitution of equation (25)-(26) into boundary condition (4) and by a suitable change of symbolism we lead to following expressions:

$$F_1(\sigma) + \overline{F}_1(\sigma) - \frac{\sigma^2\overline{\omega}'(\sigma)}{\omega'(\sigma)}\left[\frac{\overline{\omega}(\sigma)}{\omega'(\sigma)}F_1'(\sigma) + F_2(\sigma)\right] = \frac{E\alpha qR}{12(2\sigma^4+1)}\iota\left[18 + 5\sigma^4 - \sigma^2(6+7\sigma^2)\right] \quad (27)$$

$$F_1(\sigma) + \overline{F}_1(\sigma) - \frac{\sigma^2\overline{\omega}'(\sigma)}{\omega'(\sigma)}\left[\frac{\overline{\omega}(\sigma)}{\omega'(\sigma)}F_1'(\sigma) + F_2(\sigma)\right] = \frac{E\alpha qR\sigma^5}{12(2\sigma^4+1)}\iota\left[-\left(18 + \frac{5}{\sigma^4}\right) + \frac{1}{\sigma^2}\left(\sigma + \frac{7}{\sigma^4}\right)\right] \quad (28)$$

The boundary of the hole is free from external load therefore logarithmic terms in relation (5)-(6) vanishes. The function $F_1(w)$ and $F_2(w)$ appearing in stress components given in equation 18(a)-18(b) are in the form

$$F_1(w) = a_1(w) + \sum_{k=0}^{\infty} a_{-k}w^{-k} \quad (29)$$

$$F_2(w) = b_1 w + \sum_{k=0}^{\infty} b_{-k}w^{-k} \quad (30)$$

The equation (28) after some manipulation and integrate in each case over the circumference of the unit circle $|w| = 1$ and after a lengthy calculation leads to the following equations:

$$F_1(w)(1+2w^4) = a_1 w(1+2w^4) + 2a_0 w^4 + 2a_{-1}w^3 + 2a_{-2}w^2 + 2a_{-3}w + 2a_{-4} - \frac{4}{3}\frac{\overline{a}_1}{w} + \frac{7E\alpha qR}{12}\iota\frac{1}{w} \quad (31)$$

$$F_1(w)(1+2w^4) = w^5\left[\begin{array}{l} 2a_1 - \frac{4}{3}\frac{\overline{a}_1}{w^6} - \overline{a}_0\left(\frac{1}{w^5} + \frac{2}{w}\right) - \frac{2}{3}\frac{\overline{a}_{-1}}{w^4} - \frac{1}{3}\frac{\overline{a}_{-2}}{w^3} + \frac{1}{3}\frac{\overline{a}_{-4}}{w} \\ + \frac{2\overline{b}_1}{w^4} + \frac{2\overline{b}_0}{w^3} + \frac{2\overline{b}_{-1}}{w^2} + \frac{2\overline{b}_{-2}}{w}\frac{E\alpha qR}{12}\iota\left(\frac{5}{w^4} - \frac{6}{w^2} - \frac{7}{w^6}\right) \end{array}\right] \quad (32)$$

Upon solving equations (31)-(32), we arrive at the desired expression for $F_1(w)$, as following:

$$F_1(w) = -\frac{1}{4}E\alpha qR\frac{\iota}{(1+2w^4)}\frac{1}{w} - \frac{w(5+6w^4)}{3} \quad (33)$$

The function $F_1(w)$ now found from equation (27), after integrating in each case over the circumference of the unit circle $|w| > 1$ and substitute $F_1(w)$ from equation (33) as:

$$F_2(w) = \frac{1}{6}E\alpha qR\frac{\iota w^3}{(1+2w^4)^3}\left[13w^2(1-2w^4) + \frac{1}{3}(36w^8 - 16w^4 + 9)\right] \quad (34)$$

Upon substituting $F_1(w)$, $F_2(w)$ into stress components

Table 1. Material parameters.

Material parameters	steel
Young modulus, E	195 × 10ψN m^{-2}.
Thermal expansion, α	17.7 × 10^{-}6℃
Tensile stress, p	860 Mpa

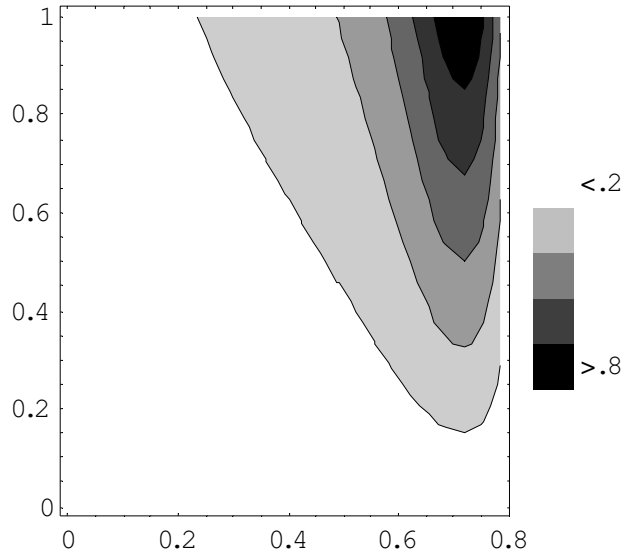

Figure 3a. $\tau_{\beta\beta}$ at $\beta = \frac{\pi}{4}$

given by 18(a)-18(b) and we obtain the following expressions for thermal stresses:

$$\tau_{\rho\rho} + \tau_{\beta\beta} = \frac{-2E\alpha qR(41 + 2Cos2\beta + 36Cos4\beta)Sin\beta}{3(5 + 4Cos4\beta)} \quad 35)$$

$$\tau_{\rho\rho} - \tau_{\beta\beta} + 2i\tau_{\rho\beta} = \frac{E\alpha qR}{3(5+4Cos4\beta)}\left[\rho^2 A + B + i(\beta\rho^2 C + D + \rho^2 E)\right] \quad (36)$$

$$A = 3771Cos2\beta + 3132Cos4\beta + 2106Cos6\beta + 1080Cos8\beta + 612Cos10\beta + 144Cos12\beta + 72Cos2\beta Cos14\beta + 2205 \quad (37)$$

$$B = -1807Sin\beta + 1911Sin3\beta + 780Sin5\beta - 828Sin7\beta + 798Sin9\beta - 796Sin11\beta + 156Sin13\beta - 144Sin15\beta \quad (38)$$

$$C = 4410 + 6264Cos4\beta + 2160Cos8\beta + 288Cos12\beta \quad (39)$$

$$D = 3203Cos\beta + 4917Cos3\beta + 348Cos5\beta + 2772Cos7\beta - 558Cos9\beta + 940Cos11\beta - 156Cos13\beta + 144Cos14\beta \quad (40)$$

$$F = 639Sin2\beta + 1026Sin6\beta + 468Sin10\beta + 72Sin14\beta \quad (41)$$

The material, steel is chosen to perform the numerical calculations. The material parameters in SI units are given

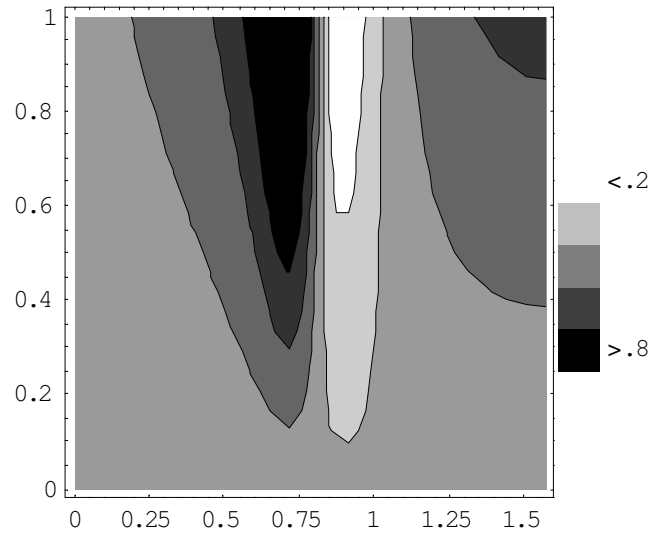

Figure 3b. $\tau_{\beta\beta}$ at $\beta = \frac{\pi}{2}$

in Table 1.

Figures 3a-3c illustrate the stress component $\tau_{\rho\rho}$ versus angle β and it is observed that contour lines are symmetric. Also, contour graphs for stress component

$$\tau_{\beta\beta}, \tau_{\rho\rho} + \tau_{\beta\beta} \text{ and } \sqrt{(\tau_{\rho\rho})^2 + (\tau_{\beta\beta})^2}$$

for different values of angle β, are shown in Figures 4a-4c, Figures 5a-5c and Figures 6a-6c. for a plate with a square hole with rounded corners. The pattern of contour lines observed in these cases is also symmetric. On the contour of the square hole, the stress component $\tau_{\beta\beta}$ becomes an azimuthal component. The expression for the azimuthal stress is obtained as following:

$$\tau_{\beta\beta} = \frac{2E\alpha qR}{3(5 + 4Cos4\beta)}(5Sin\beta - Sin3\beta) \quad (42)$$

Figures 7a-7c, shows the contour graph for the azimuthal stress $\tau_{\beta\beta}$, on the square hole with rounded corner and the radius of curvature ρ^* of the rounded corner of square is taken as $\rho_{\beta=45^o} = \frac{1}{10}R = \frac{3}{50}a$.

The equation (1) for $n = 2$, and ($a \neq b$) represent an elliptical hole. To study this case we consider an infinite plate of unit thickness with an elliptic hole and the conditions under isothermal conditions. A uniform tensile stress p applied at infinity to be stretch in y-direction and the geometry of the problem is shown in Figure 2.

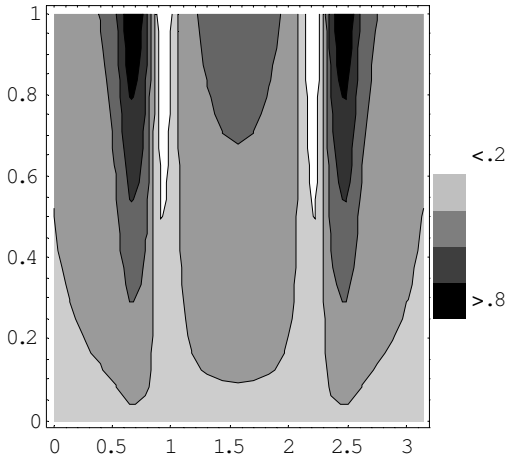

Figure 3c. $\tau_{\beta\beta}$ at $\beta = \pi$

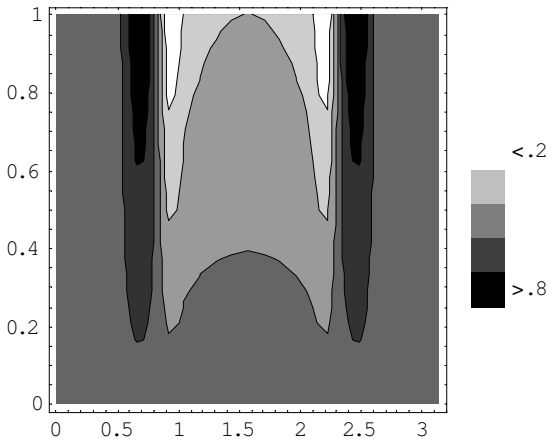

Figure 4c. $\tau_{\rho\rho}$ at $\beta = \pi$.

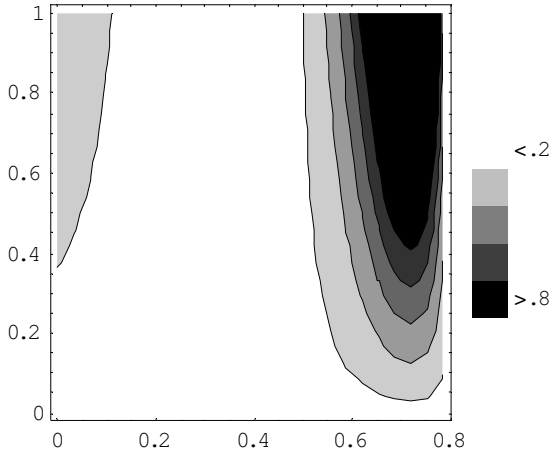

Figure 4a. $\tau_{\rho\rho}$ at $\beta = \frac{\pi}{4}$.

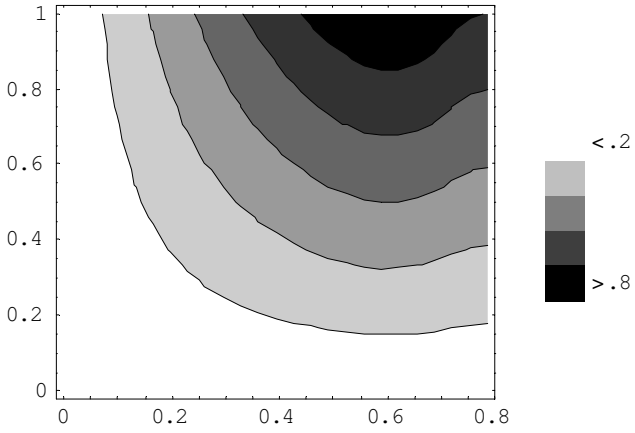

$\tau_{\rho\rho} + \tau_{\beta\beta}$ at $\beta = \frac{\pi}{4}$

Figure 5a

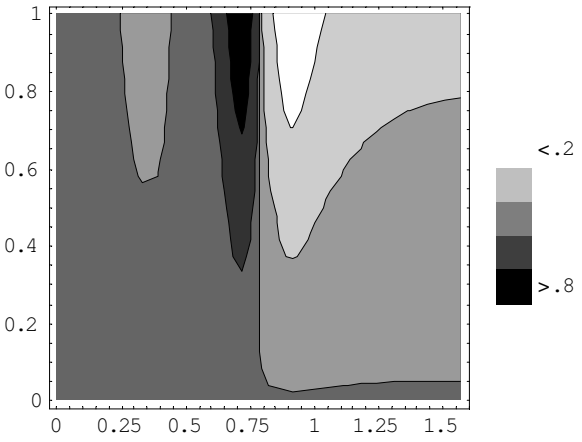

Figure 4b. $\tau_{\rho\rho}$ at $\beta = \frac{\pi}{2}$.

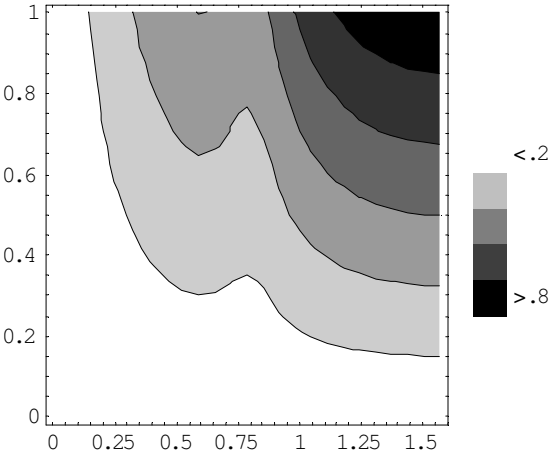

Figure 5b. $\tau_{\rho\rho} + \tau_{\beta\beta}$ at $\beta = \frac{\pi}{2}$.

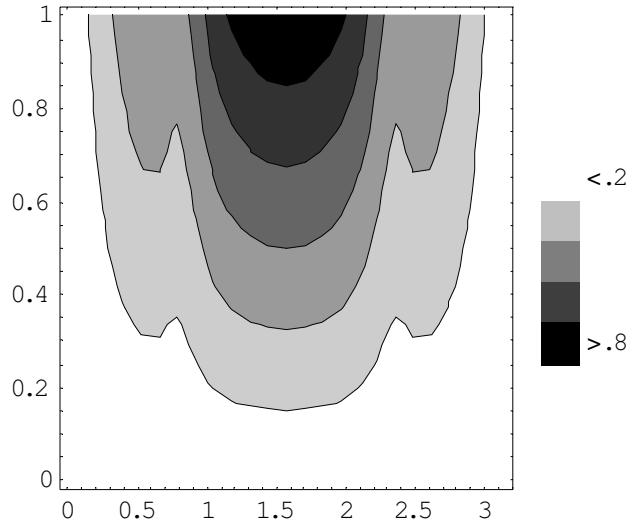

Figure 5c. $\tau_{\rho\rho} + \tau_{\beta\beta}$ at $\beta = \pi$.

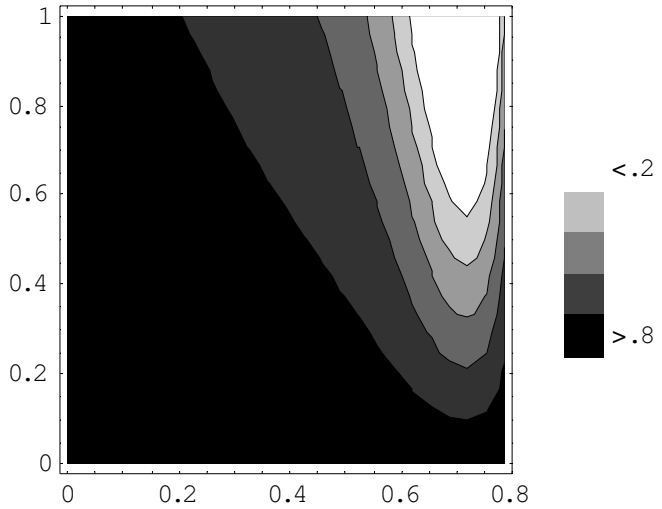

Figure 6a. $\sqrt{(\tau_{\rho\rho})^2 + (\tau_{\beta\beta})^2}$ at $\beta = \frac{\pi}{4}$.

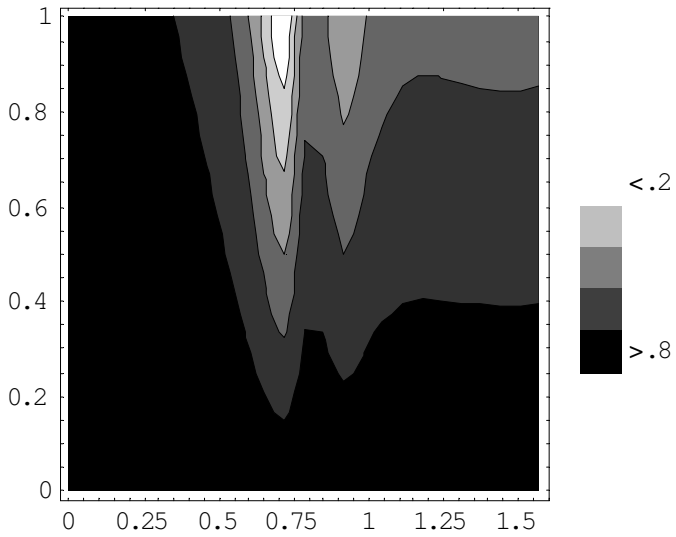

Figure 6b. $\sqrt{(\tau_{\rho\rho})^2 + (\tau_{\beta\beta})^2}$ at $\beta = \frac{\pi}{2}$.

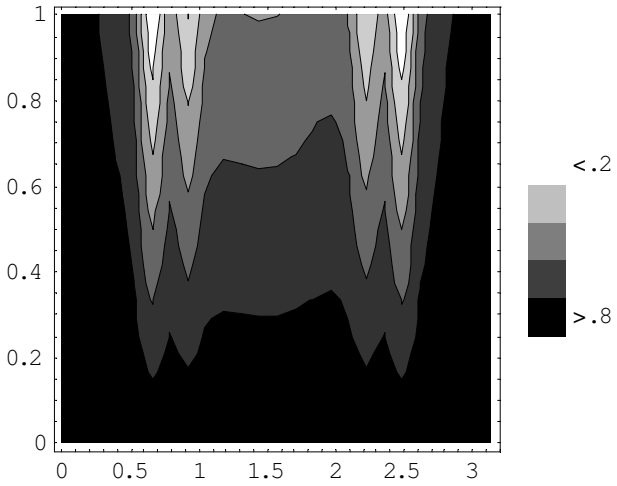

Figure 6c. $\sqrt{(\tau_{\rho\rho})^2 + (\tau_{\beta\beta})^2}$ at $\beta = \pi$

The mapping function given by equation (12) in this case is:

$$z = \omega(w) = R\left(w + \frac{m}{w}\right) \qquad (43)$$

This function maps the exterior of an ellipse onto the exterior of the unit circle. The parameter

$$R = \frac{a+b}{2}, \quad m = \frac{a-b}{a+b} \qquad (44)$$

Where;

$$a = R(1+m), \qquad b = R(1-m) \qquad (45)$$

Assuming there is no load acting on the contour of the hole, and the conditions are isothermal, after replacing $\chi'(z)$ by $\psi(z)$, equation (3) becomes

$$\psi_1(z) + z\psi_1'(z) - \overline{\psi}(z) = 0 \qquad (46)$$

On the boundary $\sigma = 1e^{\iota\beta}$ in *w*- plane and the equation (47) takes the form or explicitly,

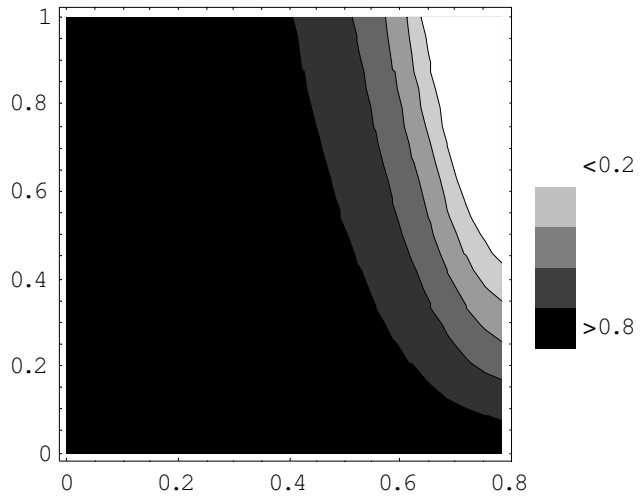

Figure 7a. Azimuthal stresses $\tau_{\beta\beta}$ at $\beta = \frac{\pi}{4}$.

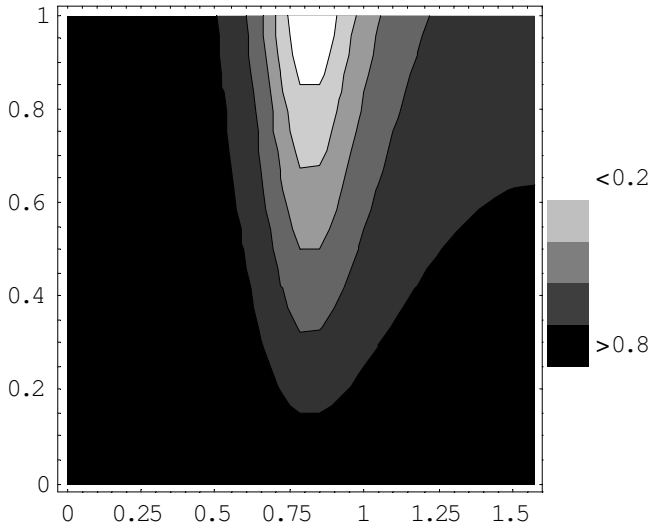

Figure 7b. Azimuthal stresses $\tau_{\beta\beta}$ at $\beta = \frac{\pi}{2}$.

$$\psi_1(\sigma) + \frac{\omega(\sigma)}{\overline{\omega}'(\sigma)}\psi_1'(\sigma) + \overline{\psi}(\sigma) = 0 \tag{47}$$

Equation (48) and its conjugate become

$$\psi_1(\sigma) + \frac{1}{\sigma}\frac{\sigma^2 + m}{1 - m\sigma^2}\overline{\psi}_1'(\sigma) + \overline{\psi}(\sigma) = 0 \tag{48}$$

$$\overline{\psi}_1(\sigma) + \sigma\frac{1 + m\sigma^2}{\sigma^2 - m}\psi_1'(\sigma) + \psi(\sigma) = 0 \tag{49}$$

Where;

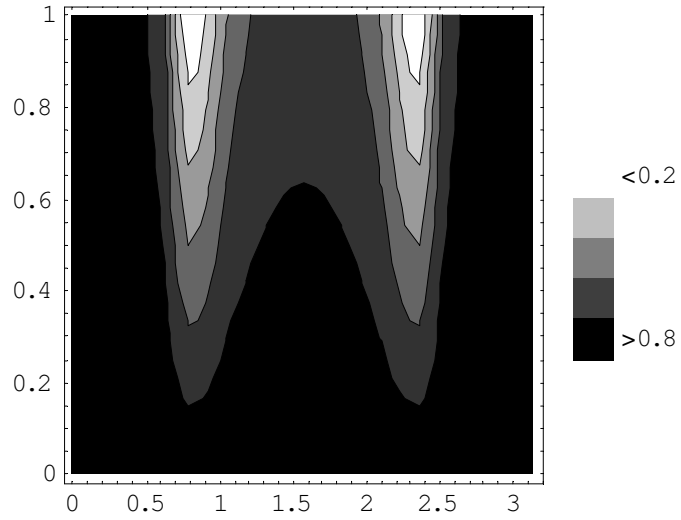

Figure 7c. Azimuthal stresses $\tau_{\beta\beta}$ at $\beta = \pi$.

$$\frac{\omega(\sigma)}{\overline{\omega}'(\sigma)} = \frac{1}{\sigma}\frac{\sigma^2 + m}{1 - m\sigma^2}, \qquad \frac{\overline{\omega}(\sigma)}{\omega'(\sigma)} = \sigma\frac{1 + m\sigma^2}{\sigma^2 - m} \tag{50}$$

Upon setting $P_x = P_y = 0$ in equations (4)-(5), take the following form:

$$\phi_1(w) = R(B + \imath C)w + \phi^*(w) \tag{51}$$

$$\psi(w) = R(B' + \imath C)w + \psi^*(w) \tag{52}$$

Where; $\phi^*(w)$ and $\psi^*(w)$ are analytic functions. Further equation (51)-(52) assume the form:

$$\phi^*(\sigma) + \frac{1}{\sigma}\frac{\sigma^2 + m}{1 - m\sigma^2}\overline{\phi}^{*\prime}(\sigma) + \overline{\psi}^*(\sigma) = -\frac{pR}{4}\left(\sigma + \frac{1}{\sigma}\frac{\sigma^2 + m}{1 - m\sigma^2} + \frac{2}{\sigma}\right) \tag{53}$$

$$\overline{\psi}^*(\sigma) + \sigma\frac{1 + m\sigma^2}{\sigma^2 - m}\overline{\phi}_1^{*\prime}(\sigma) + \psi^*(\sigma) = -\frac{pR}{4}\left(\frac{1}{\sigma} + \sigma\frac{1 + m\sigma^2}{\sigma^2 - m} + 2\sigma\right) \tag{54}$$

Upon solving the equation 2(a)-2(b) in integral form involving integrals taken over the circle and after some manipulation we find

$$\tau_{xx} + \tau_{yy} = p\frac{\rho^4 + 2\rho^2 Cos2\beta - 2m - m^2}{\rho^4 - 2m\rho^2 Cos2\beta - 2m + m^2} \tag{55}$$

$$\tau_{yy} - \tau_{xx} + 2\imath\tau xy = p\left[\begin{array}{l} 1 - \frac{1+m}{(w^2-m)^3}\left\{\frac{2w^2}{\overline{w}}(w^2+m) + (w^2-m)(mw^2-1)\right\} \\ + \frac{1+m}{(w^2-m)}\left\{\frac{2w^2(1+mw^2)}{(w^2-m)^2} + 1\right\} \end{array}\right] \tag{56}$$

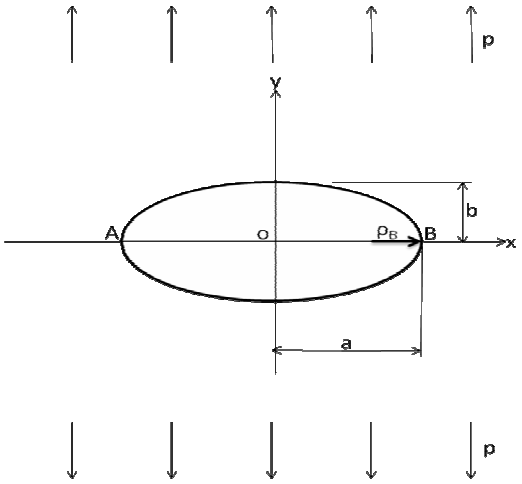

Figure 8. The geometry of the problem.

Where; $w = e^{i\beta}$ and the expressions for thermal stress components are obtained as:

$$\tau_{xx} = A' + d\left(B'Cos\beta + C'Cos2\beta + D'Cos3\beta + E'Cos4\beta + F'Cos5\beta + G'Cos6\beta\right) \quad (57)$$

$$\tau_{yy} = A' - d\left(B'Cos\beta + C'Cos2\beta + D'Cos3\beta + E'Cos4\beta + F'Cos5\beta + G'Cos6\beta\right) \quad (58)$$

$$A' = \frac{1}{2}\left[\frac{p\left(\rho^4 + 2\rho^2 Cos2\beta - 2m - m^2\right)}{\rho^4 - 2m\rho^2 Cos2\beta + m^2}\right] \quad (59)$$

$$B' = -2 + 5m - 26m^2 - 4m^3 - 16m^4 - 7m^5 + 4m^2\left(3 - m - m^2 + 3m^3\right) \quad (60)$$

$$C' = -2 + 27m + 2m^2 + 35m^3 + 6m^4 + 5m^5 + 2m^6 \quad (61)$$

$$D' = -12m - 8m^2 + 4m^3\left(1 - m - m^2\right) + 2m^6 \quad (62)$$

$$E' = -6 - 2m - 18m^2 - 2m^3 - 4m^4 + 2m^5 \quad (63)$$

$$F' = 4\left(1 + m\right) \quad (64)$$

$$G' = m\left(2 + 3m^2\right) \quad (65)$$

$$d = \frac{1}{2}\left[\frac{p}{2\left(1 + m^2 - 2mCos2\beta\right)^3}\right] \quad (66)$$

The material parameters given by equation (42) are used to draw the contour graphs for stress system in the plate of stainless steel with an elliptical hole. Figures 8a - 8c shows the stress component τ_{xx} versus angle β and the contour lines in each Figure are for parameter *m* where *m* varies from 0.2 - 1. Similarly, contour graphs for stress

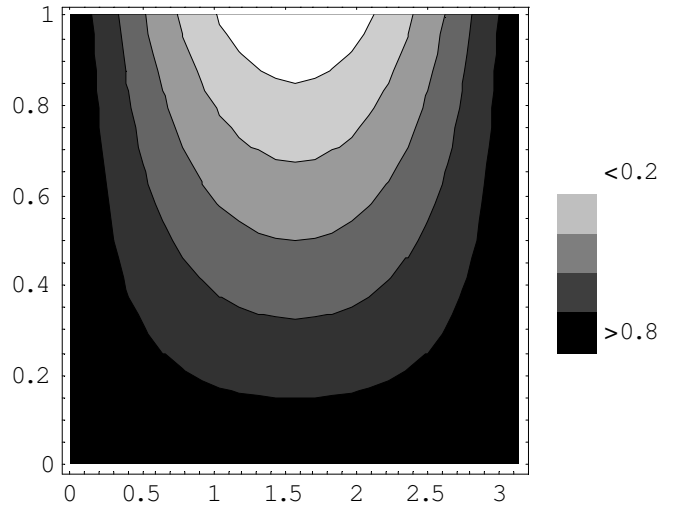

Figure 8a. τ_{xx} at $\beta = \frac{\pi}{4}$.

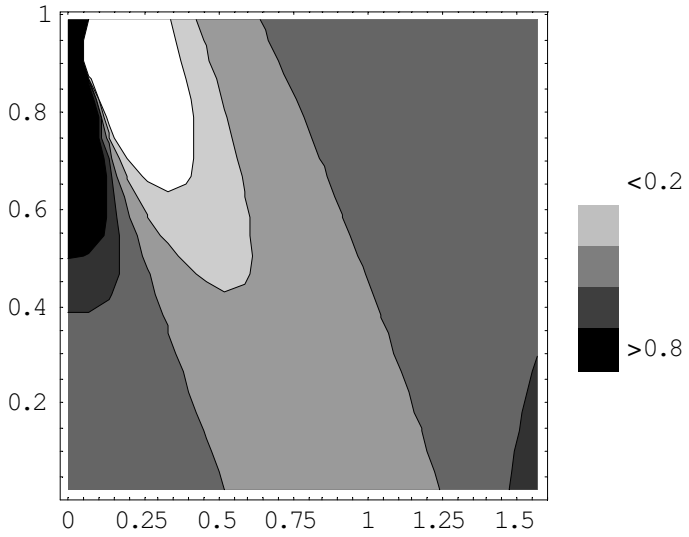

Figure 8b. τ_{xx} at $\beta = \frac{\pi}{2}$.

component $\tau_{yy}, \tau_{xx} + \tau_{yy}$ and $\sqrt{(\tau_{xx})^2 + (\tau_{yy})^2}$ for different values of angle β, are depicted and are shown in Figures 9a-9c,10a - 10c and 11a -11c respectively. The symmetric behavior is noticed in all cases. The hoop stress τ_{yy} at the tips A and B of the major axis (Figure 2), is evaluated from equation (55) for $\beta = 0$ and $\rho = 1$, is

$$\tau_{yy\max} = p\left(1 + 2\frac{a}{b}\right) \quad (67)$$

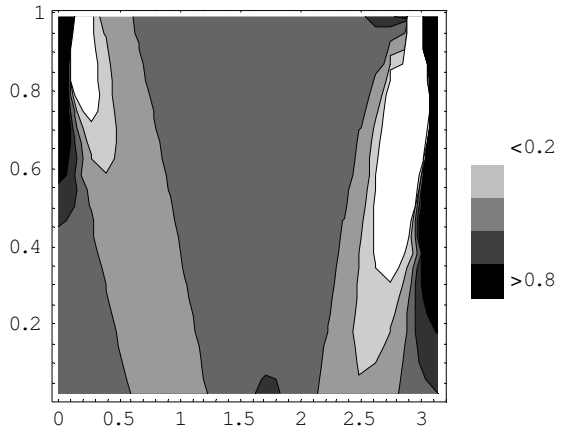

Figure 8c. τ_{xx} at

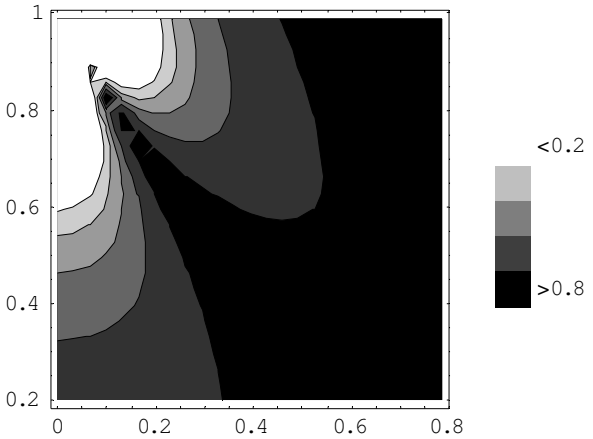

Figure 9a. τ_{yy} at $\beta = \frac{\pi}{4}$.

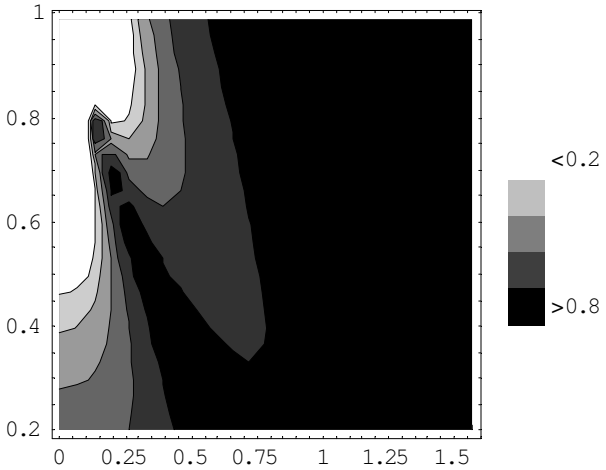

Figure 9b. τ_{yy} at $\beta = \frac{\pi}{2}$.

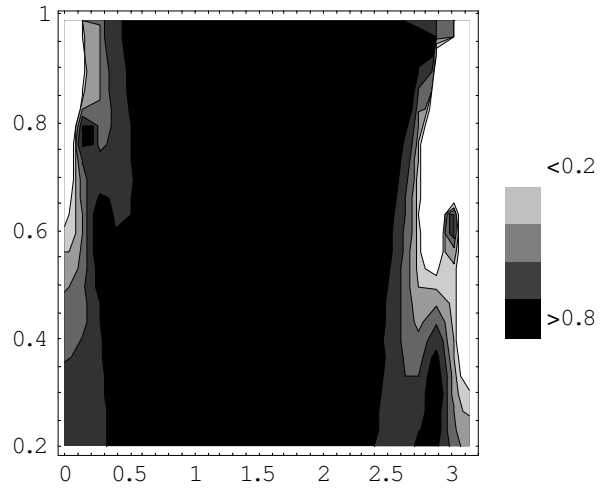

Figure 9c. τ_{yy} at $\beta = \pi$.

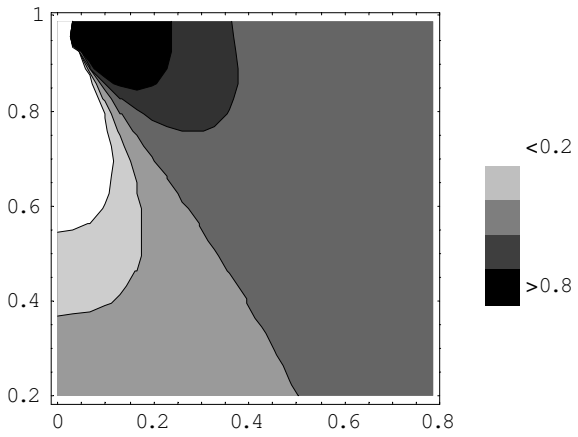

Figure 10a. $\tau_{xx} + \tau_{yy}$ at $\beta = \frac{\pi}{4}$.

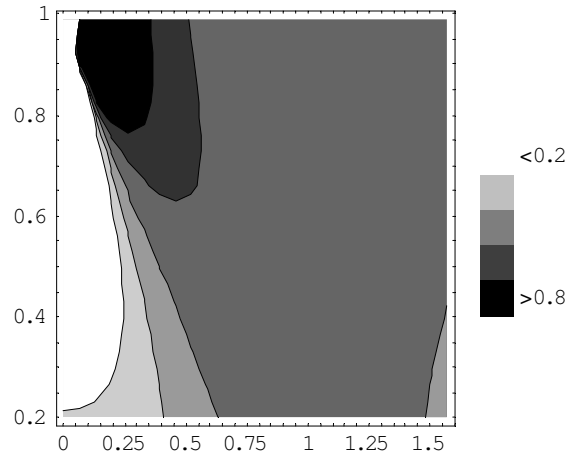

Figure 10b. $\tau_{xx} + \tau_{yy}$ at $\beta = \frac{\pi}{2}$.

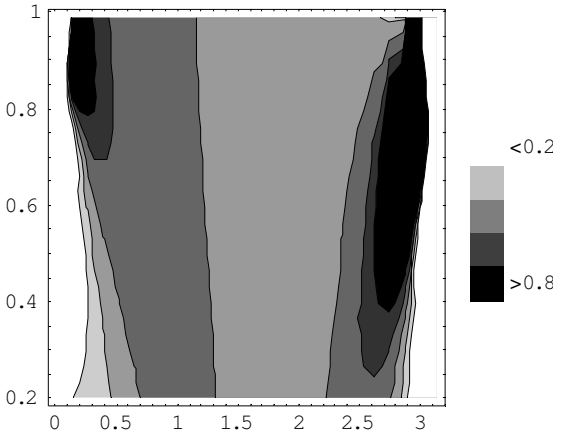

Figure 10c. $\tau_{xx} + \tau_{yy}$ at $\beta = \pi$

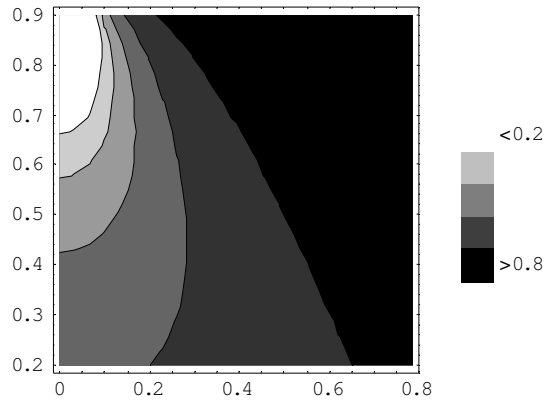

Figure 11a. $\sqrt{(\tau_{xx})^2 + (\tau_{yy})^2}$ at $\beta = \frac{\pi}{4}$.

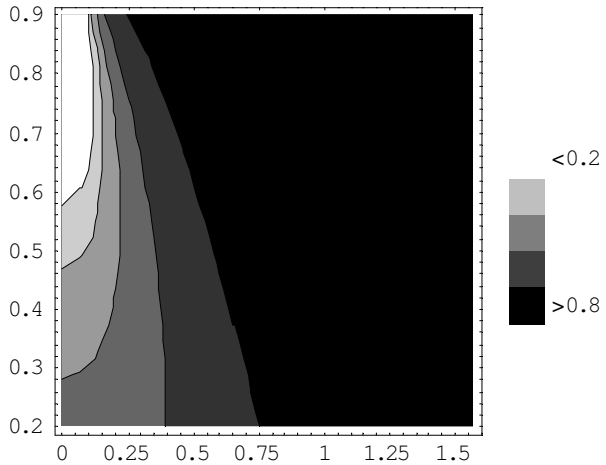

Figure 11b. $\sqrt{(\tau_{xx})^2 + (\tau_{yy})^2}$ at $\beta = \frac{\pi}{2}$.

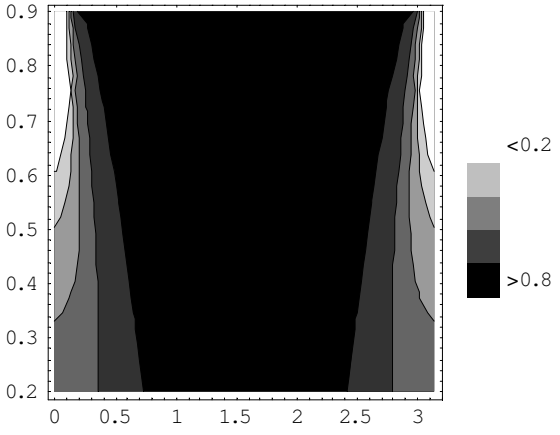

Figure 11c. $\sqrt{(\tau_{xx})^2 + (\tau_{yy})^2}$ at $\beta = \pi$.

The radius of curvature of an ellipse at a point *x,y* is:

$$\rho_{x,y} = a^2 b^2 \left(\frac{x^2}{a^4} + \frac{y^2}{b^4} \right)^{\frac{3}{2}} \tag{68}$$

Hence, at the point $A(x = a, y = 0), \rho_A = \frac{b^2}{a}$, and equation (67) becomes:

$$\tau_{yy\max} = p\left(1 + 2\sqrt{\frac{a}{\rho_A}}\right) \tag{69}$$

The maximum stress $\tau_{yy\max}$ is shown in Figure 11d. The contour lines are bundled in the beginning, then scattered.

The equation (44), for m = 0 and *R* = a, represents a circular hole. In this case stress components are computed as:

$$\tau_{xx} = \frac{p}{2}\left[\left(-1 + \frac{2}{\rho^2}\right)Cos2\beta - 3Cos4\beta + 2Cos5\beta\right] \tag{70}$$

$$\tau_{yy} = \frac{p}{2}\left[\left(-1 + \frac{2}{\rho^2}\right)Cos2\beta + 3Cos4\beta - 2Cos5\beta\right] \tag{71}$$

By using the data given by equation (42) in Figures 12a - 12c to Figures 15a - 15c set of $\tau_{xx}, \tau_{yy}, \tau_{xx} + \tau_{yy}$ and $\sqrt{(\tau_{xx})^2 + (\tau_{yy})^2}$ versus angle β for different values of ρ that is ρ varies from 0.2 - 1 for a plate of steel with circular hole. 5.2(b) the equation. (44) In the limiting case $b \to 0$, represents a slit of length 2a = 4*R* and the expressions for stress components in this

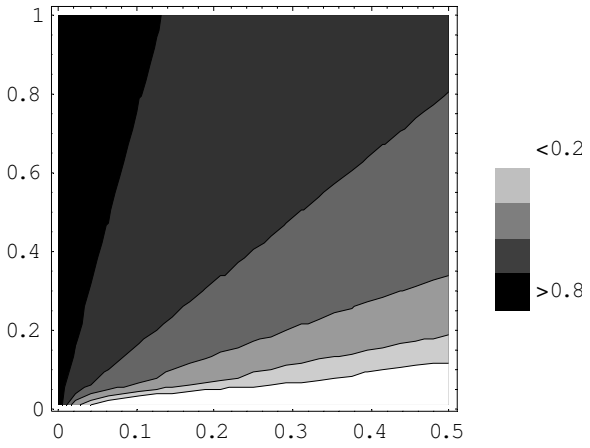

Figure 11d. The hoop stress τ_{yy} at the tip of the major axis.

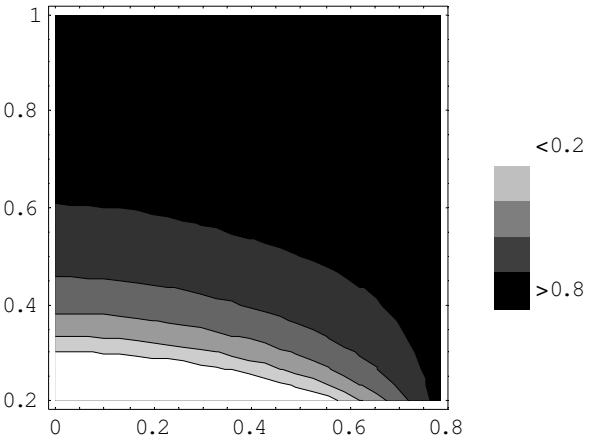

Figure 12a. τ_{xx} at $\beta = \frac{\pi}{4}$.

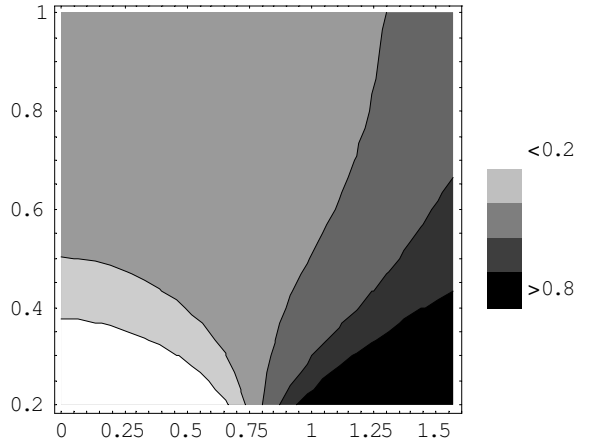

Figure 12b. τ_{xx} at $\beta = \frac{\pi}{2}$.

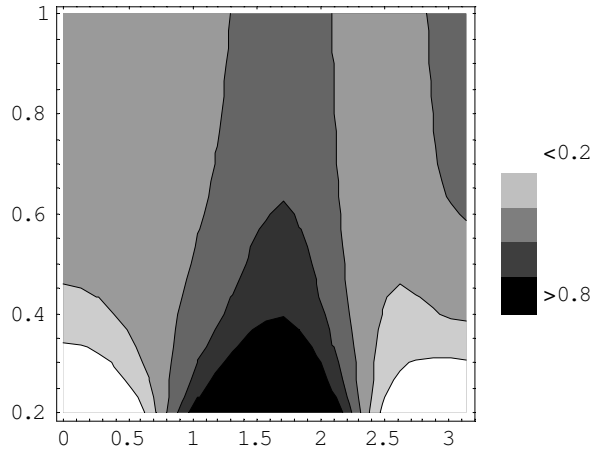

Figure 12c. τ_{xx} at $\beta = \pi$.

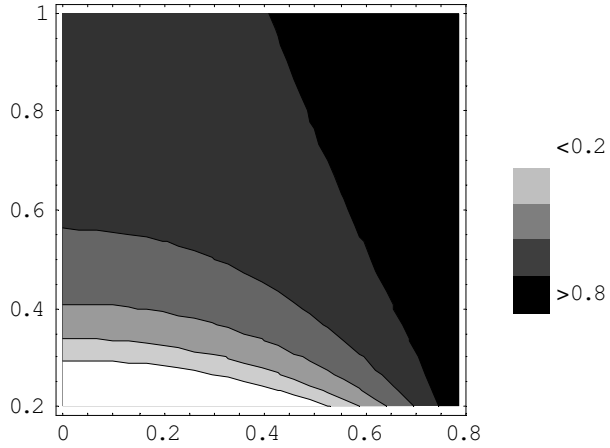

Figure 13a. τ_{yy} at $\beta = \frac{\pi}{4}$.

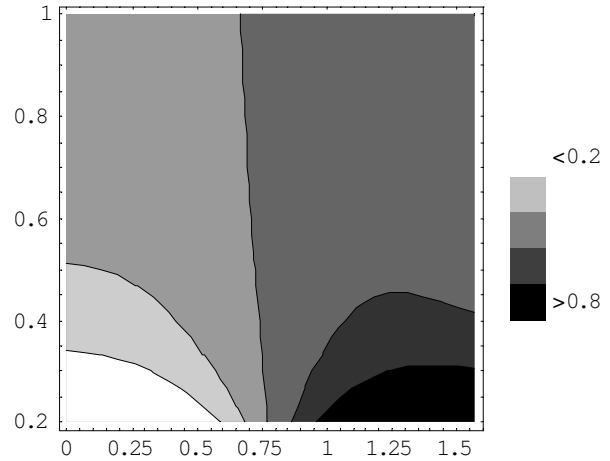

Figure 13b. τ_{yy} at $\beta = \frac{\pi}{2}$.

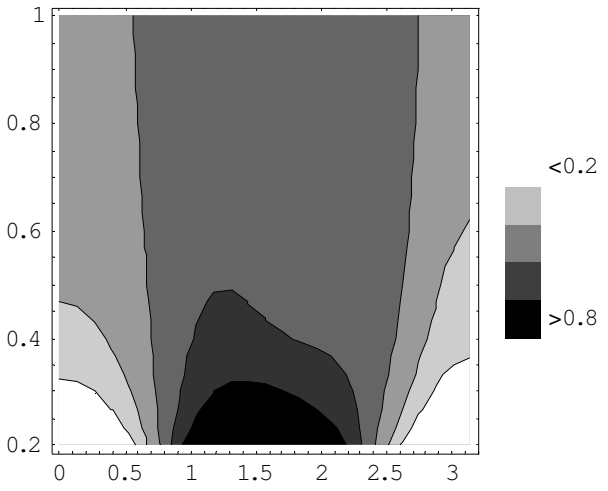

Figure 13c. τ_{yy} at $\beta = \pi$.

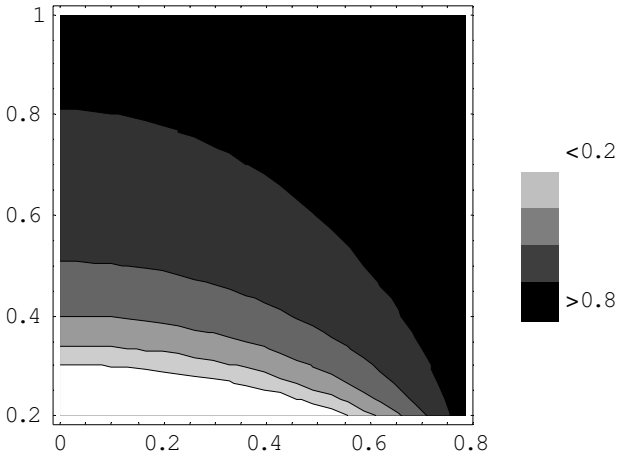

Figure 14a. $\tau_{xx} + \tau_{yy}$ at $\beta = \frac{\pi}{4}$.

case are:

$$\tau_{xx} = \frac{1}{2}\left[\frac{-5p}{4} + \frac{p\left(-3+\rho^4+2\rho^2 Cos5\beta\right)}{\rho^2} + pCot\beta Csc\beta\right] \quad (72)$$

$$\tau_{yy} = \frac{1}{2}\left[\frac{-5p}{4} + \frac{p\left(-3+\rho^4+2\rho^2 Cos5\beta\right)}{\rho^2} - pCot\beta Csc\beta\right] \quad (73)$$

Figures 16a -16b to Figures 19a -19b are depicted to show the variation in stress system for a plate with a slit. It is seen that for $\rho_A \to 0$, in equation (69), the stress at the ends of the major axis of the ellipse goes to infinity and ellipse degenerates into a razor-thin slit of length *2a,* the tips of the slit are points at which material starts to

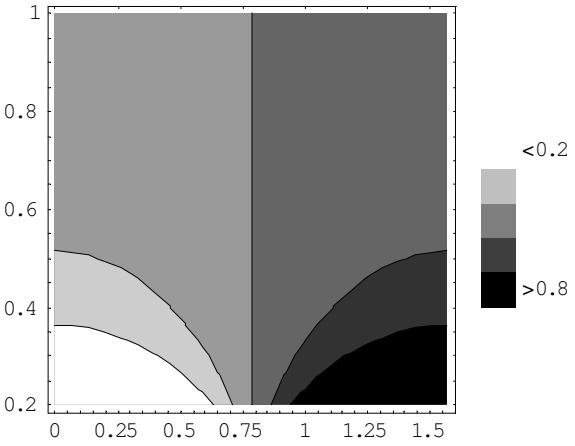

Figure 14b. $\tau_{xx} + \tau_{yy}$ at $\beta = \frac{\pi}{2}$.

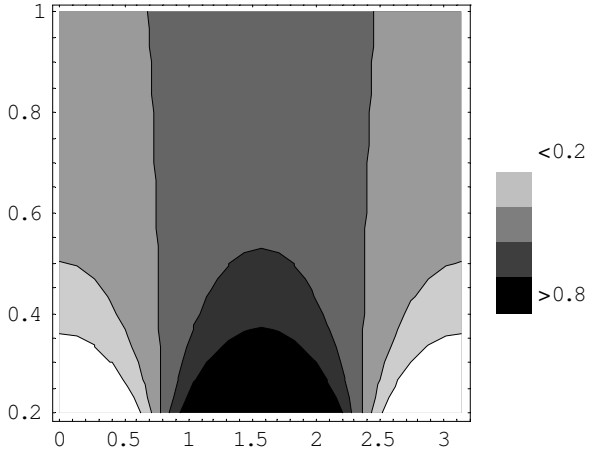

Figure 14c. $\tau_{xx} + \tau_{yy}$ at $\beta = \pi$.

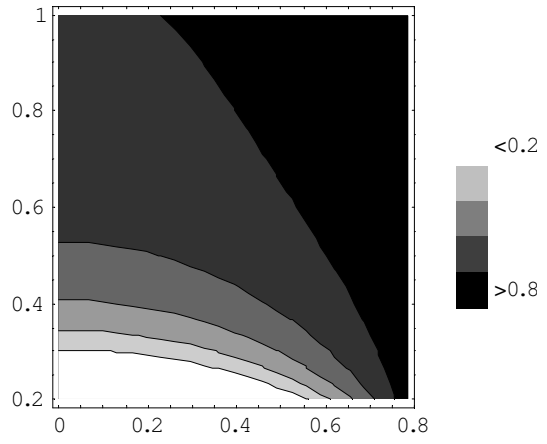

Figure 15a. $\sqrt{(\tau_{xx})^2 + (\tau_{yy})^2}$ at $\beta = \frac{\pi}{4}$.

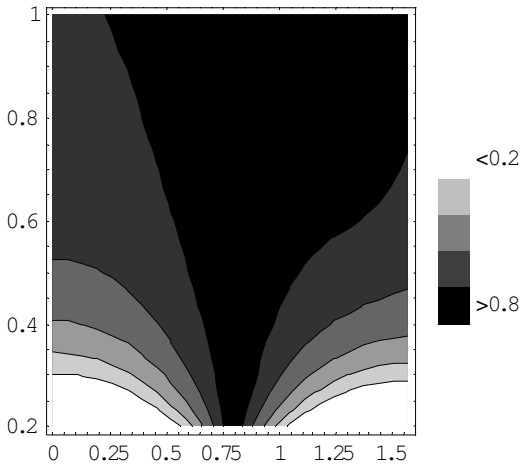

Figure 15b. $\sqrt{(\tau_{xx})^2 + (\tau_{yy})^2}$ at $\beta = \frac{\pi}{2}$.

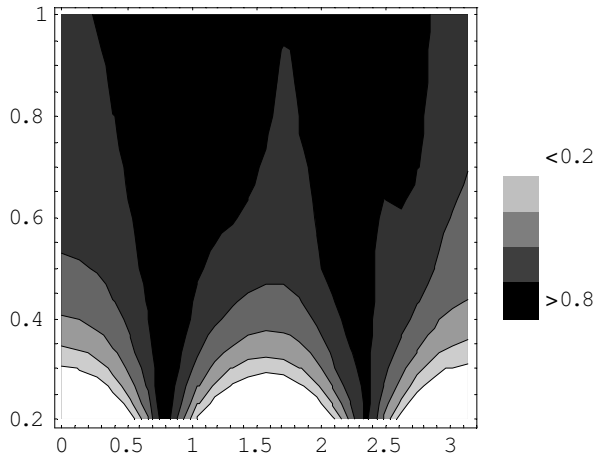

Figure 15c. $\sqrt{(\tau_{xx})^2 + (\tau_{yy})^2}$ at $\beta = \pi$.

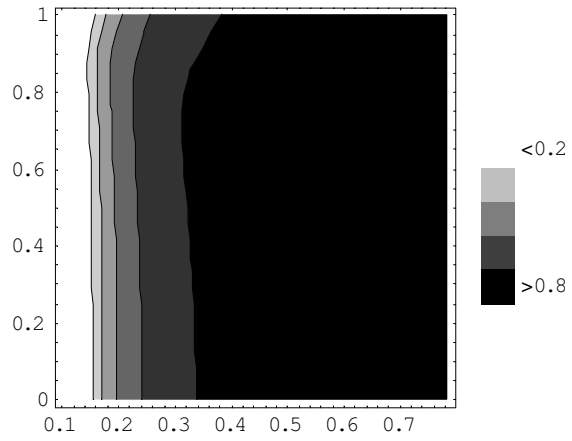

Figure 16a. τ_{xx} at $\beta = \frac{\pi}{4}$.

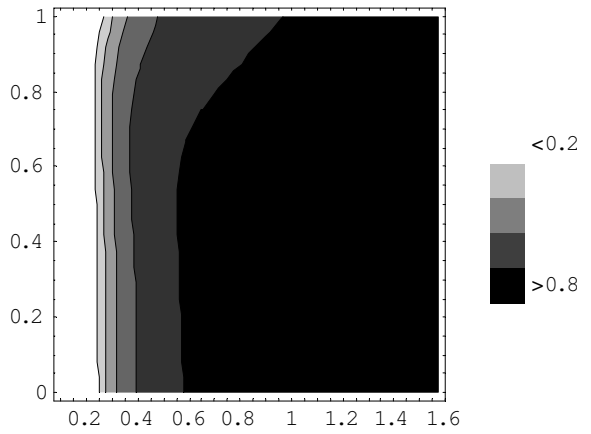

Figure 16b. τ_{xx} at $\beta = \frac{\pi}{2}$.

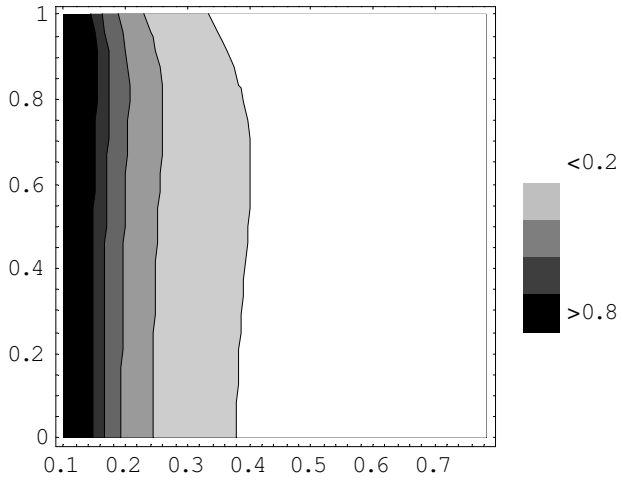

Figure 17a. τ_{yy} at $\beta = \frac{\pi}{4}$.

yield or undergoes a brittle fracture. It should be emphasized that these highly hazardous effects of sharp slits occur independently of the magnitude of the `tensile stress or length of the slit. A thin slit represents a type of a crack. Further *β=0, w=ρ* on the prolongation of the major axis of the ellipse to the right (Figure 2). On the account of the symmetry $\tau_{xy} = 0$ and in the case of slit *m→1*, then equations (55) - (56) gives:

$$\tau_{xx} + \tau_{yy} = p\left(\frac{3+\rho^2}{\rho^2 - 1}\right) \tag{74}$$

$$\tau_{yyx} - \tau_{xx} = p \tag{75}$$

Upon solving equations (75) - (76) on the prolongation of

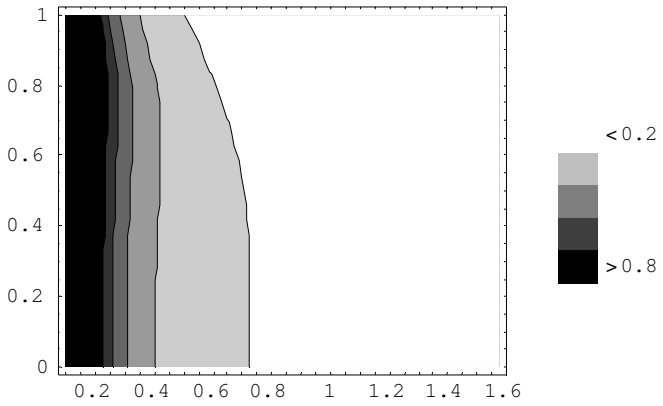

Figure 17b. τ_{yy} at $\beta = \frac{\pi}{2}$.

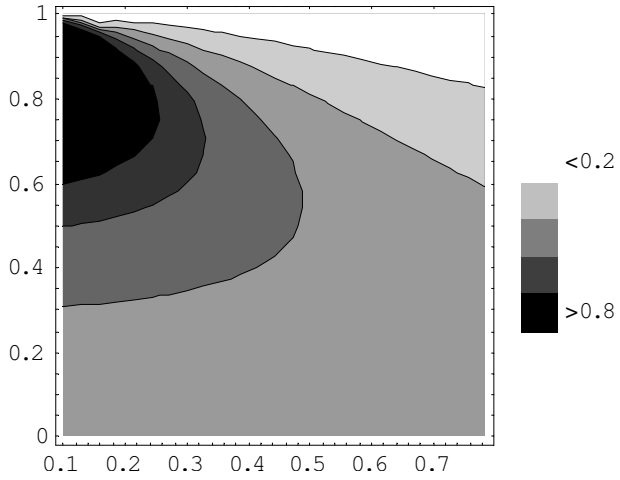

Figure 18a. $\tau_{xx} + \tau_{yy}$ at $\beta = \frac{\pi}{4}$.

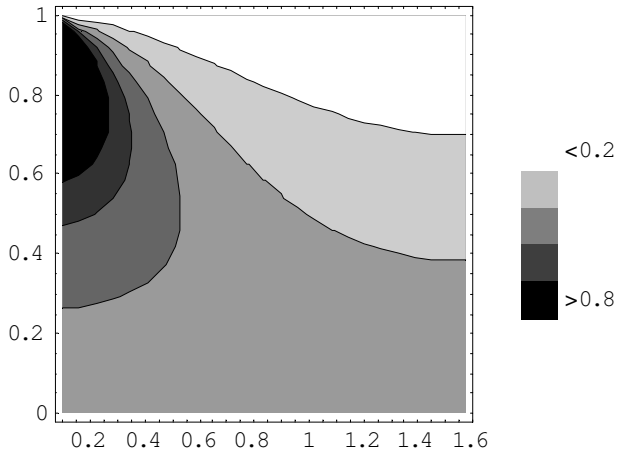

Figure 18b. $\tau_{xx} + \tau_{yy}$ at $\beta = \frac{\pi}{2}$.

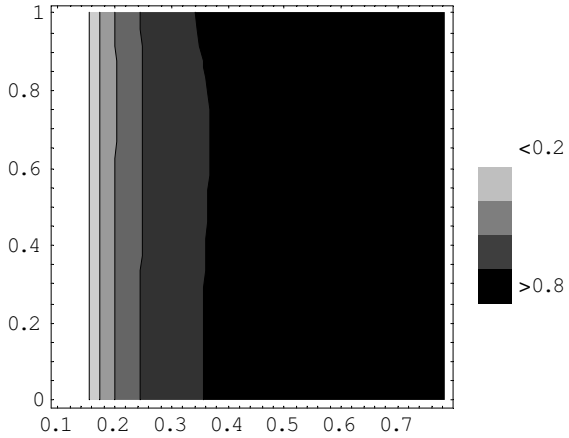

Figure 19a. $\sqrt{(\tau_{xx})^2 + (\tau_{yy})^2}$ at $\beta = \frac{\pi}{4}$.

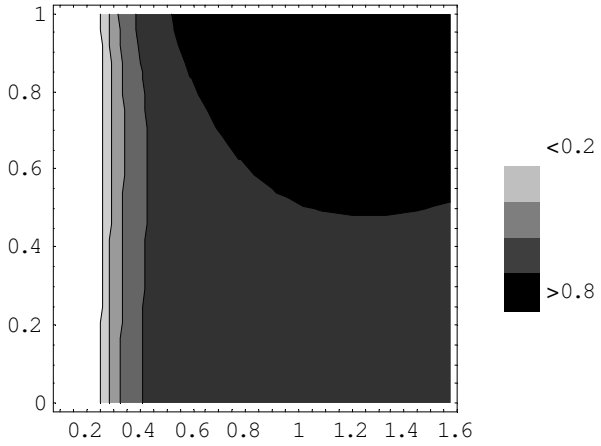

Figure 19b. $\sqrt{(\tau_{xx})^2 + (\tau_{yy})^2}$ at $\beta = \frac{\pi}{2}$.

the slit stress component is:

$$\tau_{yy} = p\left(1 + \frac{2}{\rho^2 - 1}\right) \tag{76}$$

Which shows that at the tip of the slit stress becomes unbounded. The stress system evaluated in the immediate neighborhood of the tip of the crack is following:

$$\tau_{xx} = p\sqrt{\frac{1}{2k}}Cos\frac{\alpha}{2}\left(1 - Sin\frac{\alpha}{2}Sin\frac{3\alpha}{2}\right) + ..., \tag{77}$$

$$\tau_{yy} = p\sqrt{\frac{1}{2k}}Cos\frac{\alpha}{2}\left(1 + Sin\frac{\alpha}{2}Sin\frac{3\alpha}{2}\right) + ..., \tag{78}$$

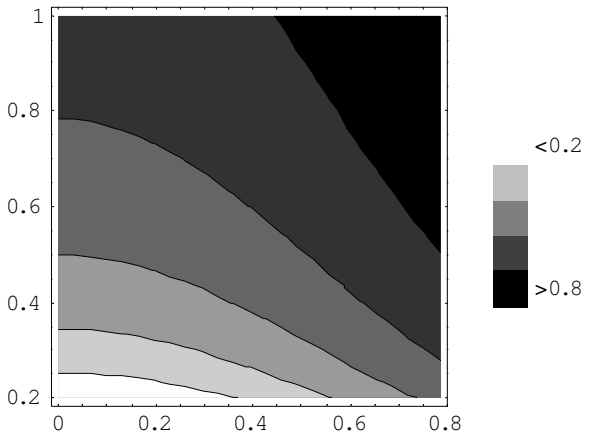

Figure 20a. τ_{xx} at $\beta = \frac{\pi}{4}$.

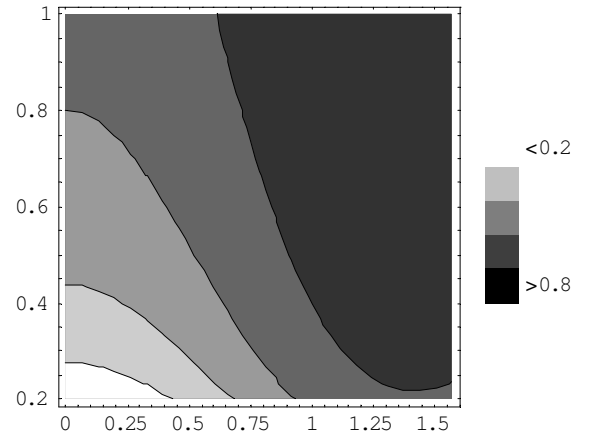

Figure 20b. τ_{xx} at $\beta = \frac{\pi}{2}$.

The stresses $\tau_{xx}, \tau_{yy}, \tau_{xy}, \tau_{xx} + \tau_{yy}$ and $\sqrt{(\tau_{xx})^2 + (\tau_{yy})^2}$ versus angle α for different values of k varies from 0.2 - 1.for a plate of steel by using data given by equation (42) in the immediate neighborhood of the tip of the crack is shown in Figures 20a - 20c to Figures 24a - 24c. The pattern of variation observed is symmetric in all cases.

Concluding Remarks

A thermal stress system around a hyperelliptical hole is studied in state of plane stress. First, the problem of an unbounded plate with a "square" hole with smoothly rounded corners is discussed. Second, a problem of an infinite plate with an elliptic hole and the particular case

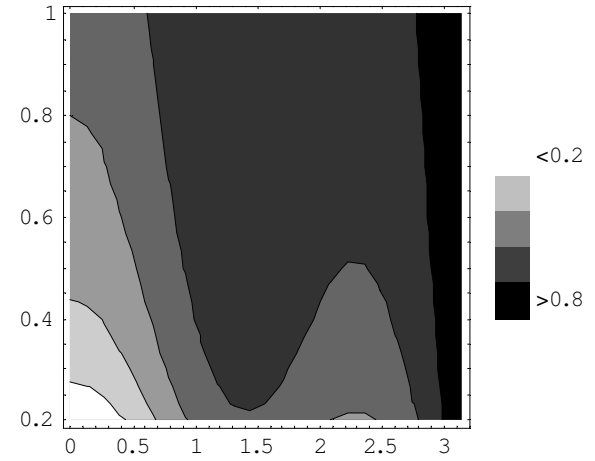

Figure 20c. τ_{xx} at $\beta = \pi$.

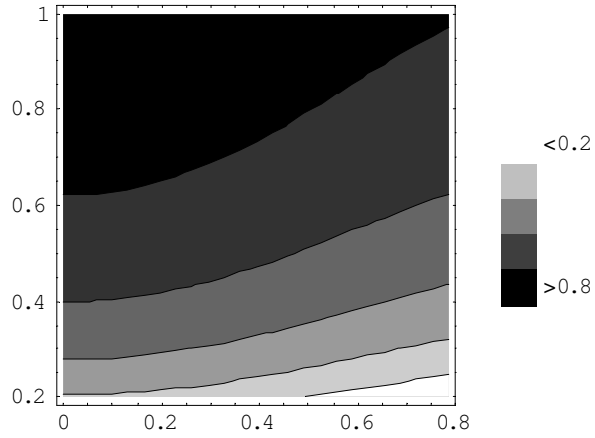

Figure 21a. τ_{yy} at $\beta = \frac{\pi}{4}$.

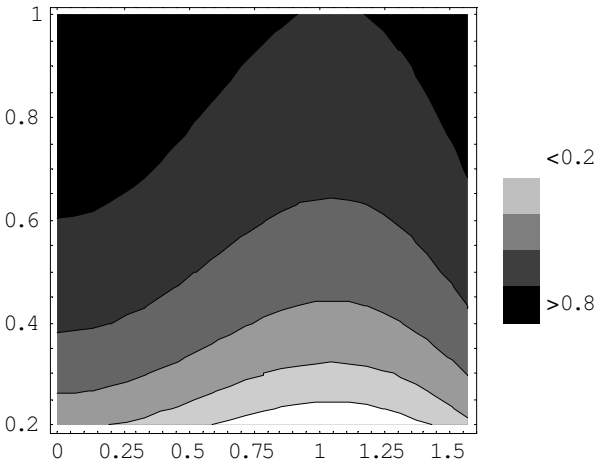

Figure 21b. τ_{yy} at $\beta = \frac{\pi}{2}$.

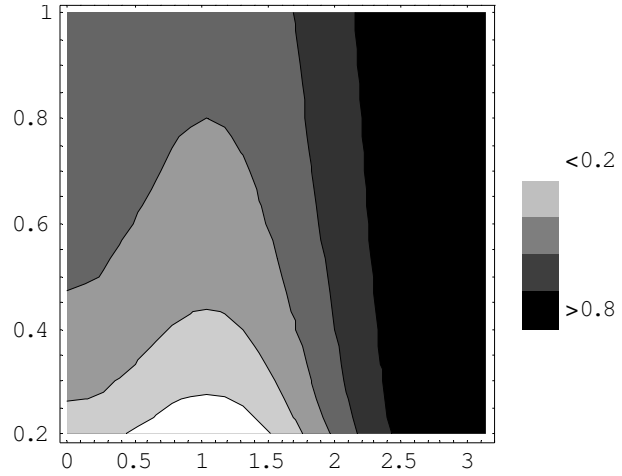

Figure 21c. τ_{yy} at $\beta = \pi$.

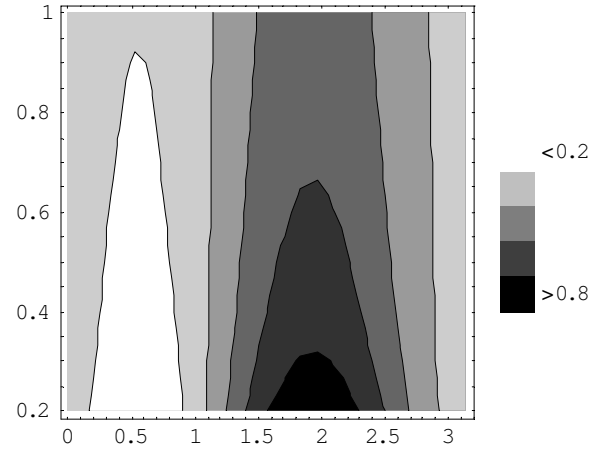

Figure 22c. τ_{xy} at $\beta = \pi$.

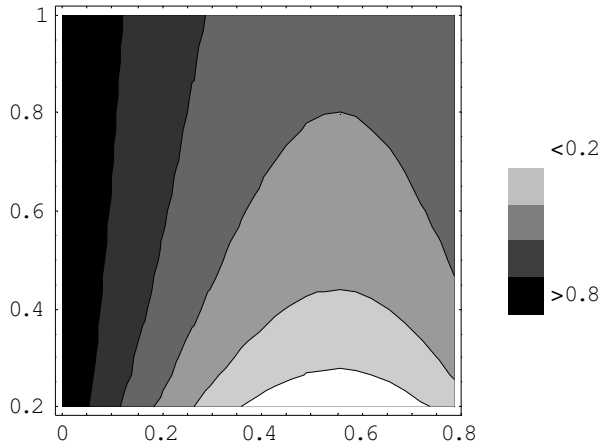

Figure 22a. τ_{xy} at $\beta = \frac{\pi}{4}$.

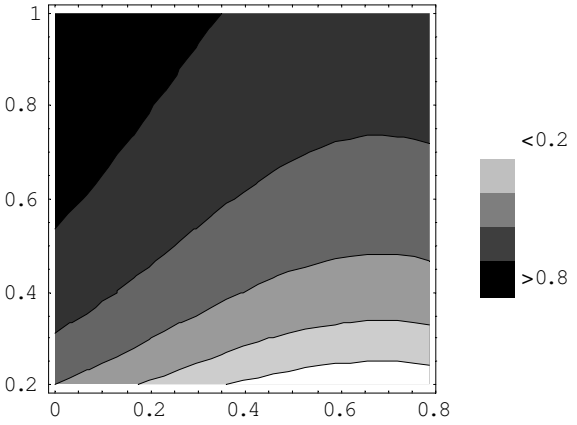

Figure 23a. $\tau_{xx} + \tau_{yy}$ at $\beta = \frac{\pi}{4}$.

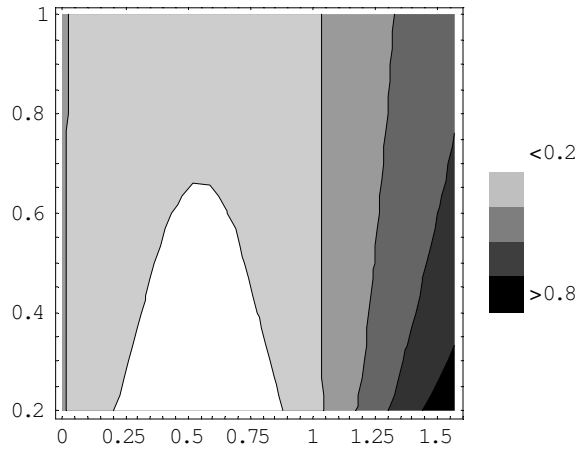

Figure 22b. τ_{xy} at $\beta = \frac{\pi}{2}$.

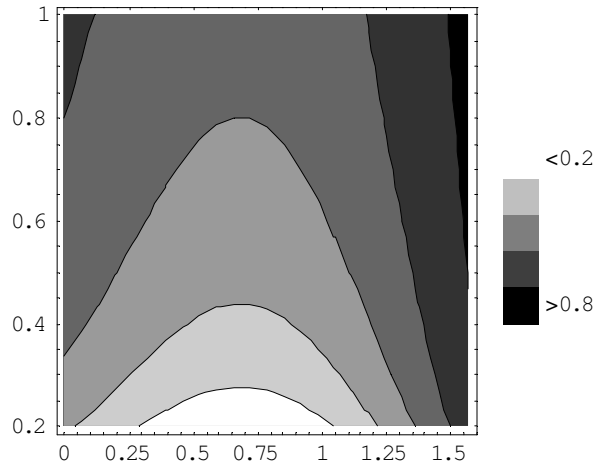

Figure 23b. $\tau_{xx} + \tau_{yy}$ at $\beta = \frac{\pi}{2}$.

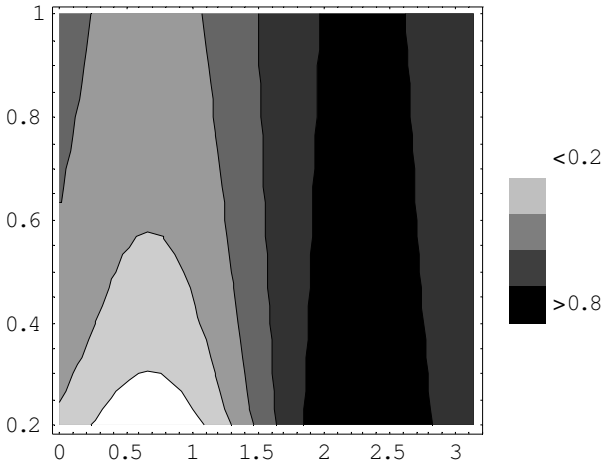

Figure 23c. $\tau_{xx} + \tau_{yy}$ at $\beta = \pi$.

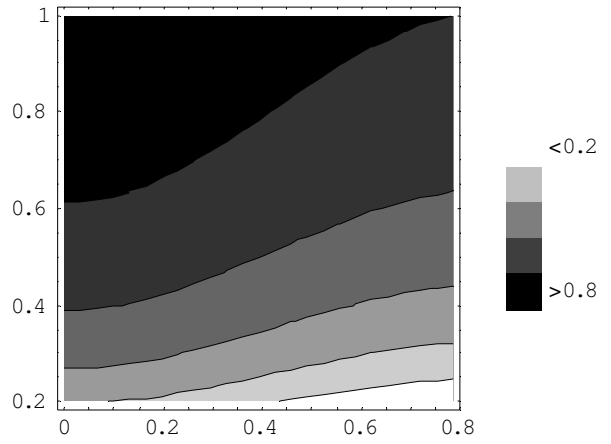

Figure 24a. $\sqrt{(\tau_{xx})^2 + (\tau_{yy})^2}$ at $\beta = \frac{\pi}{4}$.

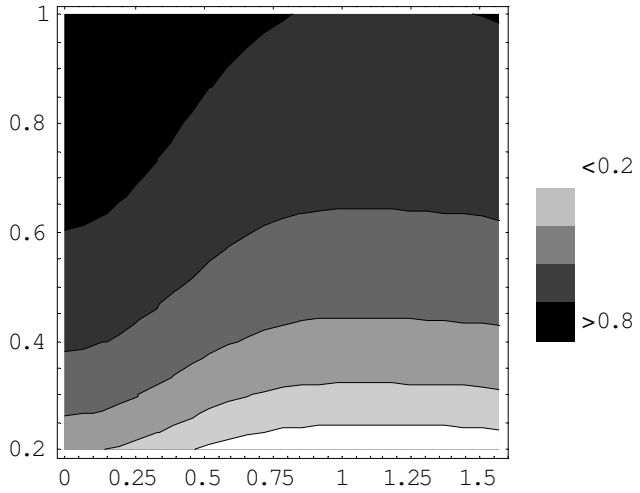

Figure 24b. $\sqrt{(\tau_{xx})^2 + (\tau_{yy})^2}$ at $\beta = \frac{\pi}{2}$.

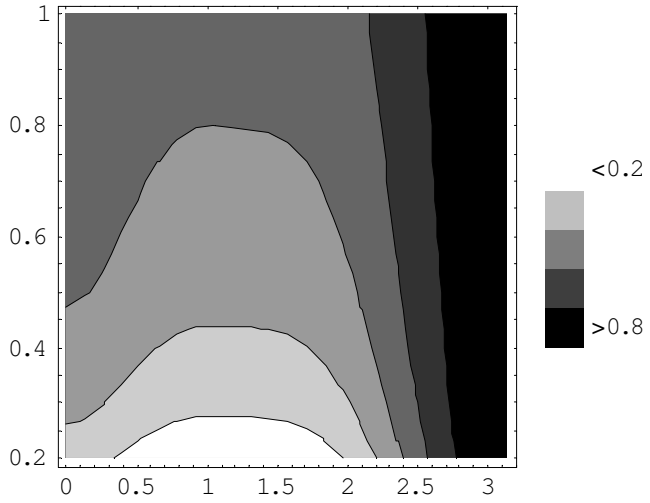

Figure 24c. $\sqrt{(\tau_{xx})^2 + (\tau_{yy})^2}$ at $\beta = \pi$.

when an elliptical hole degenerates a circular hole and a slit are has been solved by complex variable method. Obtained are analytical solutions for components of stresses, azimuthal stresses, hoop stresses, stress system in the neighborhood tip of a slit under the isothermal conditions. The variation in stresses of steel material is discussed. It is found that, the flatter the ellipse, then the larger will be the hoop stress. Further, the stress at the ends of the major axis of the ellipse goes to infinity and ellipse degenerates into a razor-thin slit of length 2a, the tips of the slit are points at which material starts to yield or undergoes a brittle fracture and these highly hazardous effects of sharp slits occur independently of the magnitude of the tensile stress or length of the slit. Also, at the tip of the slit stress becomes unbounded. The pattern of variation in stress system observed in the most cases is symmetric.

REFERENCES

Abdou MA, Aseeri SA (2009). Goursat functions for an infinite plate with a generalized curvilinear hole in ς-plane Applied Mathematics and Computation, available online Feb. 2009.

Bhullar SK (2006). Thermal stresses in a hexagon regions with an elliptic hole, J. Nonlinear Dyn. Syst. Theory 6(3): 245-256.

Chao CK, Gao B (2001). Mixed boundary-value problems of two-dimensional anisotropic thermoelasticity with elliptic boundaries, Int. J. Solids Struct. 38(34-35): 5975-5994.

Chen FM, Chao CK (2008).Stress analysis of an infinite plate with a coated elliptic hole under a remote uniform heat flow, J. Therm. Stresses 31: 599-613.

Florence AL, Goodier JN (1959). Thermal stress at spherical cavities and circular holes in uniform heat flow, J. Appl. Mech. 26: 293-294.

Florence AL, Goodier JN (1960). Thermal stresses due to disturbance of uniform heat flow by an insulated ovaloid hole, J. Appl. Mech. 27: 635-639.

Florence AL, Goodier JN (1962). Thermal stresses due to disturbance of uniform flow by an insulated spheroid cavity, Proc.4th US National Congr. Appl. Mech. 1: 595-602.

Florence AL, Goodier JN (1964). The linear thermoelastic problem of

uniform heat flow disturbed by a penny-shaped insulated crack, Int. J. Eng. Sci. 1: 533-540.
Goodier JN, Florence AL (1959). Thermal stress due to disturbance of uniform heat flow by cavities and inclusions, Stanford University, Divi Eng. Mech. Tech. Rep. 120.
Goodier JN, Florence AL (1963).Thermal stresses at an insulated circular hole near the edge or an insulated plate under uniform heat flow, quart. J. Mech. Appl. Math. 16: 273-282.
Goshima T, Miyao K (1990). Transient thermal stress in an infinite plate with a hole due to rotating heat source, J. Therm. Stresses 13, Issue 1, pp 43-56.
Hoffman RE, Ariman T (1970). Thermal bending of plates with circular holes, Nucl. Eng. Des. 14: 231-238.
Hong K, Kim J (1995). Natural mode analysis of hollow and annular elliptical cylinderical cavities, J. Sound Vib. 183(2): 327-351.
Kara A, Kanoria M (2007). Thermoelastic interaction with energy dissipation in a transversely isotropic thin circular disc, Eur. J. Mech. - A/Solids 26(6): 969-981.
Matsumoto E, Sekiya T (1982). Thermal stress of square region with an elliptical hole, Mech. Res. Commun. 9(6): 397-402.
Quinn S, Dulieu-Barton JM (2002). Determination of stress concentration factors for holes in cylinders using thermoelastic stress analysis, strain, Int. J. Exp. Mech. 38(3): 105-118.
Rao KS, Bapu Rao MN, Ariman T (1971). Thermal Stresses in Plates with Circular Holes, Nucl. Eng. Des. 15(1): 97–112.
Ukadgaonker VG, Rao DN (1999). Stress distribution around triangular holes in anisotropic plates, Compos. Struct. 45: 171-183.
Youssef HM (2009). Generalized thermoelastic infinite medium with cylindrical cavity subjected to moving heat source, Mech. Res. Commun. 36(4): 487-496.